# *Effect of temperature and magnesia on phase transformation kinetics in stoichiometric and non-stoichiometric cordierite ceramics prepared from kaolinite precursors*

**Smail Lamara, Djaida Redaoui, Foudil Sahnoune & Nouari Saheb**

**Journal of Thermal Analysis and Calorimetry**
An International Forum for Thermal Studies

ISSN 1388-6150

J Therm Anal Calorim
DOI 10.1007/s10973-018-7923-2

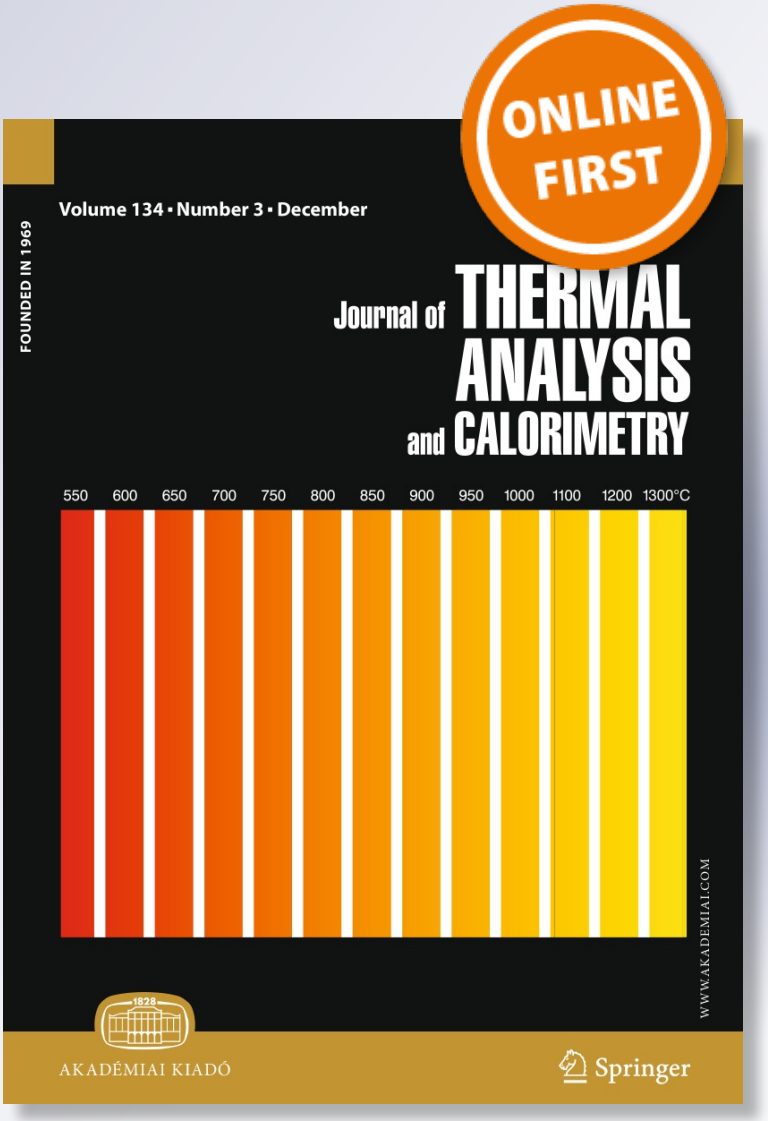


Springer

Your article is protected by copyright and all rights are held exclusively by Akadémiai Kiadó, Budapest, Hungary. This e-offprint is for personal use only and shall not be self-archived in electronic repositories. If you wish to self-archive your article, please use the accepted manuscript version for posting on your own website. You may further deposit the accepted manuscript version in any repository, provided it is only made publicly available 12 months after official publication or later and provided acknowledgement is given to the original source of publication and a link is inserted to the published article on Springer's website. The link must be accompanied by the following text: "The final publication is available at link.springer.com".

Author's personal copy

Journal of Thermal Analysis and Calorimetry
https://doi.org/10.1007/s10973-018-7923-2

# Effect of temperature and magnesia on phase transformation kinetics in stoichiometric and non-stoichiometric cordierite ceramics prepared from kaolinite precursors

Smail Lamara[1,2] · Djaida Redaoui[1,2] · Foudil Sahnoune[2,3] · Nouari Saheb[4]

Received: 24 July 2018 / Accepted: 13 November 2018
© Akadémiai Kiadó, Budapest, Hungary 2018

## Abstract

The influence of temperature and magnesia content on the formation of phases and their transformation kinetics in stoichiometric and non-stoichiometric cordierite ceramics prepared from Algerian kaolinite precursors was investigated. High-temperature X-ray diffraction was used to study the formation of phases and their transformations. Non-isothermal differential thermal analysis was used to determine kinetic parameters for the formation of $\mu$ and $\alpha$ cordierite. Activation energies were calculated by Kissinger, Boswell, and Ozawa equations. The Augis–Bennett and Matusita equations were used to calculate the mode of crystallization ($n$) and dimension of growth ($m$) parameters, respectively. The synthesized materials showed similar phase transformations, which finally led to the formation of cordierite in stoichiometric kaolinite–magnesia mixture, and cordierite along with other phases in kaolinite–magnesia mixture containing excess magnesia. The activation energy for the formation of $\alpha$ cordierite was higher than that of $\mu$ cordierite. Energies of formation of $\mu$ and $\alpha$ cordierite phases in the non-stoichiometric samples were higher than those in the stoichiometric sample. The activation energy was less sensitive to the calculation method; however, it changed significantly with MgO content. Activation energies between 573 and 964 kJ mol$^{-1}$ were obtained. Magnesia changed the crystallization mode and crystal growth dimension. The kinetic parameters $n$ and $m$, for the formation of $\mu$ or $\alpha$ cordierite, had values between 2 and 3.

**Keywords** Kaolinite · Magnesia · Cordierite · Solid-state reaction · Phase transformation kinetics

## Introduction

Cordierite phase, with $2MgO{\cdot}2Al_2O_3{\cdot}5SiO_2$ and $Mg_2Al_4Si_5O_{18}$ chemical composition and chemical formula, respectively, forms when $Al^{3+}$ and $Mg^{2+}$ cations diffuse in the $SiO_2$ structure. It is an important phase in the MgO–$Al_2O_3$–$SiO_2$ system and is characterized by a narrow sintering temperature range. Cordierite has relatively low theoretical bulk density of 2.53 g cm$^{-3}$, high melting point of 1470 °C, very low coefficient of thermal expansion ($1–2 \times 10^{-6}$ C$^{-1}$), high electrical resistivity ($> 10^{12}$ Ω cm), low thermal conductivity, high stability in harsh environments, and acceptable mechanical properties [1, 2].

Because of their thermal, electrical, and mechanical properties, cordierite ceramic materials are extensively used in many applications [1–7] including packaging, geobarometry and geothermometry [6], and thermal insulation [7]. Additionally, they are good candidates for making refractory and high thermal shock resistance products, components for turbine heat exchangers, and catalysts' supports in cars [1–5].

Although cordierite is rare in earth [8], it can be synthesized from different raw materials by different methods [9–17]. Readily available natural materials or minerals

✉ Nouari Saheb
nouari@kfupm.edu.sa

1 Physics and Chemistry of Materials Lab, Department of Physics, University Mohamed Boudiaf of M'sila, M'sila, Algeria

2 Physics Department, Faculty of Science, University Mohamed Boudiaf of M'sila, 28000, M'sila, Algeria

3 Research Unit On Emerging Materials (RUEM), University Ferhat Abbas of Sétif 01, 19000 Sétif, Algeria

4 Department of Mechanical Engineering, King Fahd University of Petroleum and Minerals, Dhahran 31261, Saudi Arabia

Published online: 30 November 2018

Author's personal copy



[7, 18–22] and reaction sintering [1, 7, 18–24] are considered the most suitable precursors and method, respectively, to synthesize low-cost cordierite ceramic materials. In some cases, additives such as NiO [25], Zn [26], $P_2O_5$ and $B_2O_3$ [27], $P_2O_5$ [28], $CeO_2$ [29], NiO and $TiO_2$ [30], BaO [31], and MgO [32, 33] are incorporated as sintering aids to facilitate cordierite formation.

The kinetics of phase transformations in cordierite ceramics [8, 25–31, 34–37] was investigated by many researchers using different method including but not limited to differential thermal analysis (DTA) [28–31, 34, 35], DSC [35, 36], and X-ray diffraction (XRD) [8, 25–27]. The kinetics parameters were evaluated from isothermal [25–27, 35] as well as non-isothermal [8, 25, 28–31, 34–37] measurements. In published works [8, 25–31, 34–37], energies for the formation of cordierite ranged from 170 to 850 kJ $mol^{-1}$.

Donald [35] used isothermal and non-isothermal DTA and DSC to analyze cordierite formation in a mixture of fine particle (particle size less than 45 μm and between 45 and 212 μm) of $Al_2O_3$, $SiO_2$, and MgO. He reported energy values in the range 532–574 and 399–426 kJ $mol^{-1}$ for the formation of $\mu$ and $\alpha$ cordierite phases, respectively. The crystallization of cordierite from $CeO_2$-free and $CeO_2$-doped glasses was investigated under non-isothermal DTA conditions [29]. Average energies of 653 and 418 kJ $mol^{-1}$ were reported for cordierite crystallization from the stoichiometric and non-stoichiometric glasses, respectively. Goel et al. [37] studied the formation of cordierite in $TiO_2$-doped MgO–$Al_2O_3$–$SiO_2$ glass by non-isothermal DTA, and found energies of 340 and 498 kJ $mol^{-1}$, for the formation of $\mu$ and $\alpha$ cordierite phases, respectively. Cordierite formation energies of 366 and 290–487 kJ $mol^{-1}$ were obtained from non-isothermal DTA measurements performed on BaO-free and BaO-doped samples, respectively [31]. Silva et al. [34] crystallized cordierite from diphasic gels. The authors performed DTA measurements under non-isothermal conditions to analyze the crystallization of cordierite and reported an energy value of 467 kJ $mol^{-1}$. The crystallization of cordierite in NiO-added glass samples was investigated by non-isothermal DTA. Energies of 300 and 500 kJ $mol^{-1}$ were obtained for the formation of $\mu$ and $\alpha$ cordierite, respectively [30]. Song et al. [36] used potassium and feldspar to prepare a glass from which cordierite was crystallized. From the non-isothermal DSC measurements, the authors obtained activation energy values between 230.77 and 279.81 kJ $mol^{-1}$ for the formation of $\alpha$ cordierite and between 348.85 and 374.33 kJ $mol^{-1}$ for the formation of $\alpha$ cordierite along with leucite.

The large variation in the reported activation energy values was attributed to the: (1) nature and composition of precursors used to obtain cordierite, (2) type of processes used to synthesize cordierite, (3) conditions under which cordierite forms, i.e., isothermal or non-isothermal, and (4) presence of sintering aids to facilitate the formation of cordierite. In previous work [38], the authors synthesized low-cost stoichiometric cordierite, from Algerian kaolinite precursors and synthetic magnesia. The objectives of this work are to synthesize stoichiometric and non-stoichiometric cordierite ceramic materials and study the influence of temperature and magnesia content on the formation of phases and their transformation kinetics. The approach is to use reaction sintering, a one-step simple heat treatment process, and naturally occurring Algerian kaolinite to produce low-cost advanced ceramic materials. The procedure involves reaction sintering two kaolinite precursors, one rich in $Al_2O_3$ and the other rich in $SiO_2$, with synthetic magnesia. Non-isothermal DTA measurements will be used to determine kinetic parameters for the formation of $\mu$ and $\alpha$ cordierite. Activation energies will be calculated by Kissinger, Boswell, and Ozawa methods. The Augis–Bennett and Matusita equations will be used to calculate the $n$ and $m$ kinetic parameters.

## Materials

The precursor materials utilized in this work were mainly two types of naturally occurring Algerian kaolinite and synthetic magnesia. The first kaolinite (abbreviated DD1) and second kaolinite (abbreviated TK) were collected from Djebel Debagh (Guelma) and Tamazarte (Jijel), respectively, in East Algeria. The composition of the two kaolinite materials is presented in Table 1. The DD1 kaolinite is made of 45.3 and 39.13 mass% silica and alumina, respectively, while the TK kaolinite contains 69.86 and 19.29 mass% of $SiO_2$ and $Al_2O_3$, respectively. The rest of oxides are present at small percentage in both materials. The DD1 and TK raw materials are suitable sources of alumina and silica and can be mixed with magnesia to synthesize cordierite which has a theoretical composition of 51.4, 34.9, and 13.8% of $SiO_2$, $Al_2O_3$, and MgO, respectively [1].

Three mixtures of DD1, TK, and MgO powders were prepared at different percentages, as shown in Table 2, to obtain stoichiometric cordierite sample (abbreviated DT00M), and two non-stoichiometric cordierite samples, abbreviated DT04M and DT08M, which after sintering contain 4 and 8 mass% MgO, respectively. Each mixture was ball-milled for 5 h and then sintered between 900 and 1350 °C for 2 h. More details on ball milling and sintering procedures are reported elsewhere [38].

Author's personal copy



**Table 1** Composition of the two kaolinite materials (mass%)

| Kaolinite | $Al_2O_3$ | $SiO_2$ | $Na_2O$ | $SO_3$ | $K_2O$ | MgO | CaO | MnO | $Fe_2O_3$ | $TiO_2$ | LOI |
|---|---|---|---|---|---|---|---|---|---|---|---|
| KT | 19.29 | 69.86 | 0.13 | 0.03 | 2.67 | 0.4 | 0.4 | – | 0.72 | 0.4 | 6.31 |
| DD1 | 39.13 | 45.30 | 0.04 | – | 0.21 | 0.05 | 0.15 | 0.02 | 0.07 | – | 14 |

**Table 2** Composition of the prepared samples (mass%)

| Samples | KT | DD1 | MgO |
|---|---|---|---|
| DT00M | 59.00 | 29.00 | 12.00 |
| DT04M | 56.33 | 27.66 | 16.00 |
| DT08M | 53.66 | 26.33 | 20.00 |

## Analytical and calculation methods

The prepared powder mixtures and sintered samples were analyzed using PANalytical (X'Pert PRO) X-ray diffraction system (Cu-Kα radiation of a wavelength 0.15418 nm). The density of the developed samples was measured by the Archimedes method using a KERN densimeter.

Non-isothermal DTA measurements were taken at room temperature to 1400 °C, at heating rates of 10, 20, 30, 40, and 50 °C $min^{-1}$, in inert environment (argon gas at a flow rate of 40 $cm^3$ $min^{-1}$). The DTA experiments were performed using a LABSYS EVO DTA/DSC-TG SETARAM instrument on samples weighing 50 mg and loaded in alumina crucibles.

The Kissinger [39, 40], Boswell [41], and Ozawa [42] methods were used to calculate the non-isothermal activation energy ($E_A$) for the formation of cordierite according to Eqs. 1, 2, and 3, respectively.

$$\ln\left(\frac{\phi}{T_p^2}\right) = -\frac{E_A}{RT_p} + C_1 \tag{1}$$

$$\ln\left(\frac{\phi}{T_p}\right) = -\frac{E_A}{RT_p} + C_2 \tag{2}$$

$$\ln(\phi) = -1.0518\frac{E_A}{RT_p} + C_3 \tag{3}$$

where $\varphi$ [°C $min^{-1}$] is the heating rate, $E_A$ [kJ $mol^{-1}$] is the energy of formation, $T_p$ [°C] is the absolute peak temperature in *DTA* curves, and $R$ is the gas constant.

The Augis–Bennett equation [43–47] was used to calculate the kinetic parameter $n$:

$$n = \frac{2,5T_p^2R}{\Delta T_p E_A} \tag{4}$$

where $\Delta T_p$ is the full width of *DTA* exothermic peak taken at its half-maximum intensity.

The modified Kissinger equation (Matusita equation) was used to calculate the kinetic parameter $m$ [44]:

$$\ln\left(\frac{\phi^n}{T_p^2}\right) = C_3 - \frac{mE_A}{RT_p} \tag{5}$$

## Results and discussion

### XRD analysis

Figure 1 shows typical XRD spectra of samples sintered at different temperatures (1000, 1100, 1200, and 1300 °C) for 2 H. The fraction of phases present in the sintered samples is presented in Fig. 2. Phases present in DT00M sample, Fig. 1a, sintered at 1000 °C were sapphirine ($Mg_{19.12}Al_{45.24}Si_{11.64}O_{80}$), quartz ($SiO_2$), and mullite ($Al_{4.5}Si_{1.5}O_{9.74}$), and their mass fractions were 30, 15, and 55 mass%, respectively. At 1100 °C, the amount of mullite decreased to 22 mass%, while the mass fractions of quartz and sapphirine increased to 26 and 52 mass%, respectively. At 1200 °C, quartz and mullite phases disappeared, the fractions of sapphirine phase increased to 79 mass%, also cristobalite and μ cordierite phases started to form, and their mass fractions were 6 and 15 mass%, respectively. At 1300 °C, only a single phase identified as α cordierite ($Mg_4Al_8Si_{10}O_{36}$) was present. XRD spectra of DT04M sample, Fig. 1b, revealed that, at 1000 °C, quartz (23 mass%), mullite (38 mass%), and sapphirine (24 mass%) were present. At 1100 °C, the magnesium silicate phase appeared (31.3 mass%), the fractions of quartz and mullite decreased to 19.2 and 10.1 mass%, respectively, and the fraction of sapphirine phase increased to 39.4 mass%. At 1200 °C, the fraction of sapphirine phase increased to 47.5 mass%, the fraction of magnesium silicate phase decreased to 17.2 mass%, and cristobalite (9 mass%) and μ cordierite (26.3 mass%) were present. At 1300 °C, α cordierite and magnesium silicate phases were present at fractions of 84 and 16 mass%, respectively. Analysis of XRD spectra of DT08M sample, Fig. 1c, showed that it is composed of 21.8 mass% magnesium silicate, 8.9 mass% quartz, 43.6 mass% mullite, and 25.7 mass% sapphirine. The mass fractions of magnesium silicate, quartz and sapphirine increased to 34, 11, and 47 mass%, respectively, with the increase in temperature to 1100 °C, while the

Author's personal copy



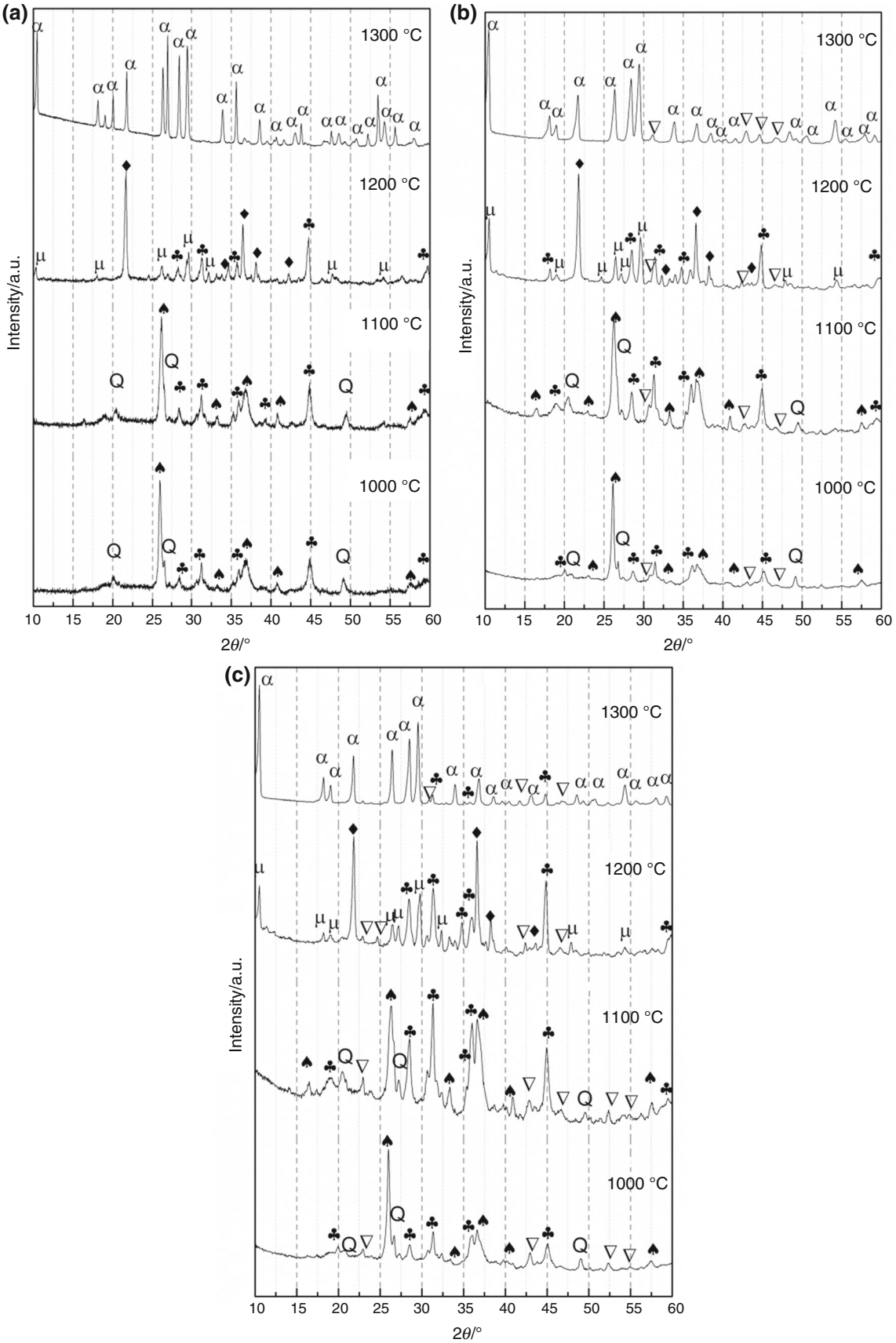

Author's personal copy



◀**Fig. 1** XRD spectra of **a** DT00M, **b** DT04M, and **c** DT08M powders sintered for 2 h. (▽: magnesium silicate ($Mg_2SiO_4$) phase, Q: quartz ($SiO_2$) phase, ♠: mullite ($Al_{4.5}Si_{1.5}O_{9.74}$) phase, ♣: sapphirine ($Mg_{19.12}Al_{45.24}Si_{11.64}O_{80}$) phase, ◆: cristobalite phase, $\mu$ and $\alpha$: allotropes of cordierite ($Mg_4Al_8Si_{10}O_{36}$))

fraction of mullite phase decreased to 8 mass%. At 1300 °C, the sample was made of magnesium silicate, sapphirine, and $\alpha$ cordierite at fractions of 22, 25 and 53 mass%, respectively.

It can be concluded, from XRD results, that the sintered samples showed similar phase transformations, which finally led to the formation of monolithic cordierite in stoichiometric kaolinite–magnesia mixture (sample DT00M), and cordierite along with other phases (magnesium silicate and sapphirine) in kaolinite–magnesia mixture with excess of magnesia (samples DT04M and DT08M). This suggests that the type, number, and amount of phases formed in cordierite ceramics strongly depend on the temperature of firing as well as the composition of starting materials. It is worth mentioning here that Njoya et al. [2] synthesized cordierite-based ceramic materials from kaolin, bauxite, and talc raw materials and reported the formation of the following: (1) cordierite as the main phase, and the absence mullite, in the mixture with large amount of talc and (2) great amount of cordierite along with mullite in the mixture which contained large amount of kaolin and less quantity of talc.

## DTA analysis

DTA curves of DT00M, DT04M, and DT08M samples recorded between room temperature and 1400 °C (at 30 °C $min^{-1}$) are shown in Fig. 3. Endothermic peaks in the range 35–290 and 500–630 °C result from adsorbed water evaporation and kaolinite dihydroxylation (formation of metakaolinite), as described by Eqs. 6 and 7, respectively.

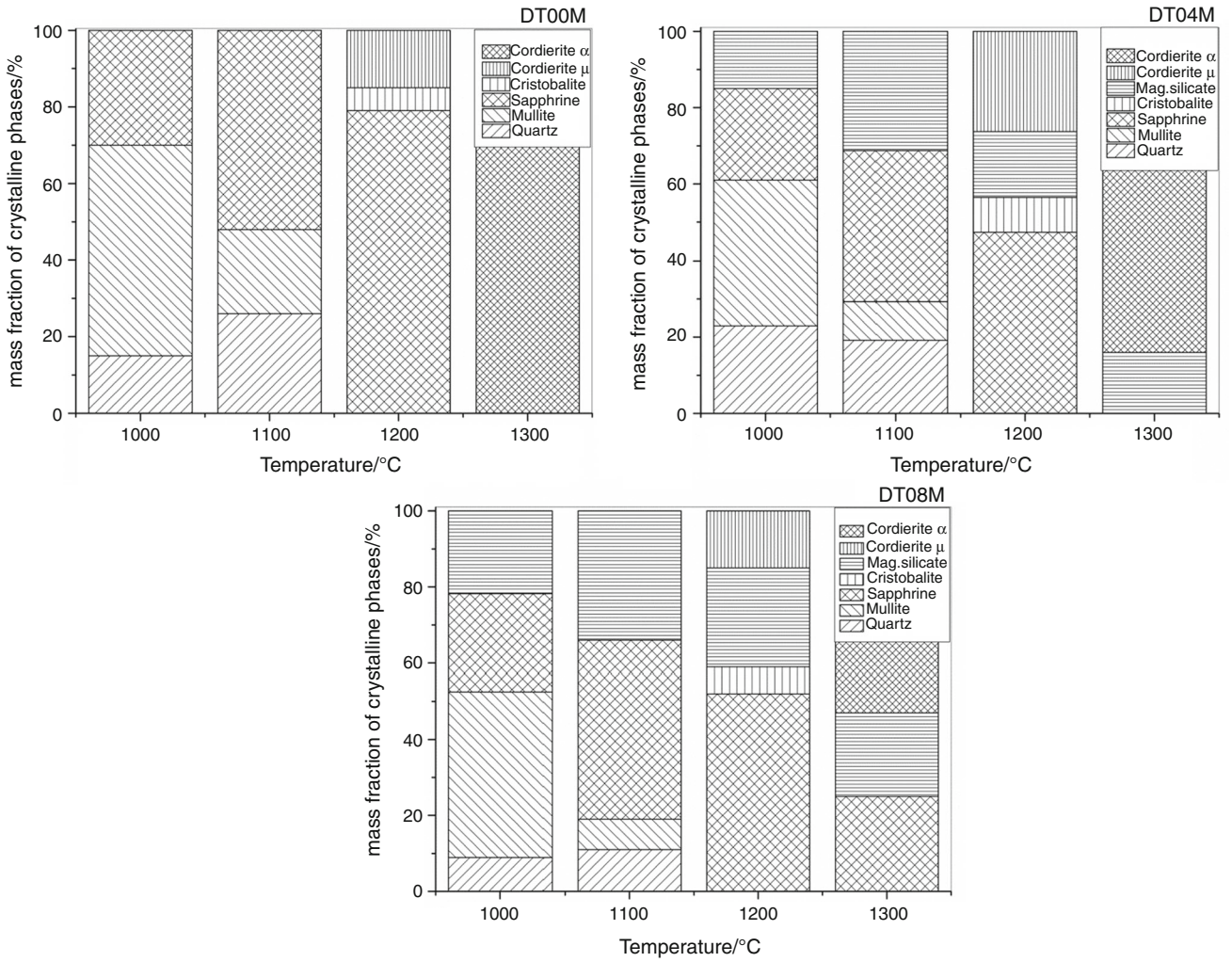


**Fig. 2** Amount of phases in sintered samples

Author's personal copy



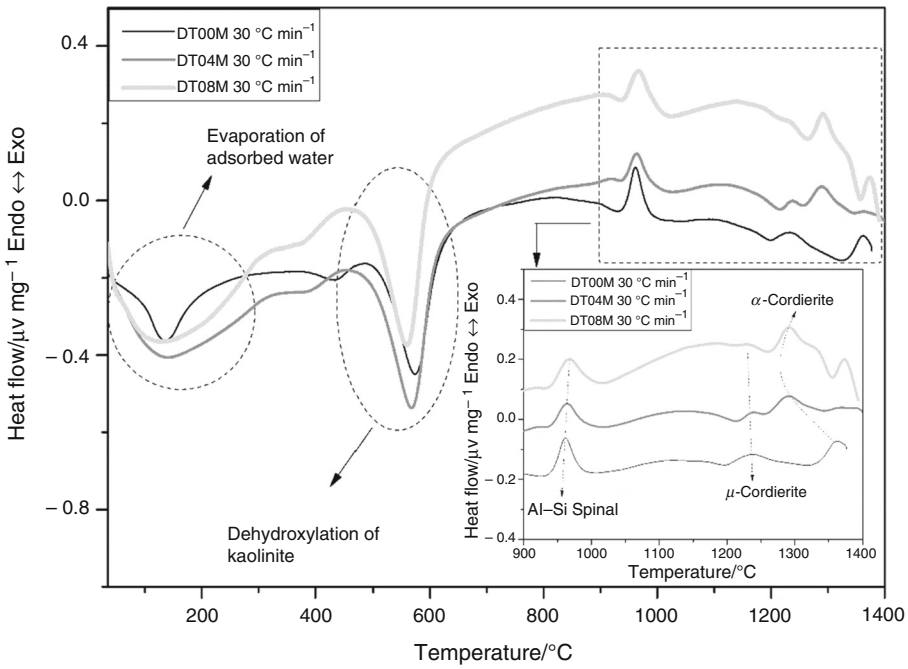


**Fig. 3** DTA curves of DT00M, DT04M, and DT08M powders heated to 1400 °C at a heating rate of 30 °C $min^{-1}$

$$29\ \text{mass\%}\ \text{KT(Tamazarte kaolin)} + 59\ \text{mass\%}\ \text{DD1}\ \text{(Djebel Debagh kaolin)} + X(X = 12,\ 16\ \text{and}\ 20)\text{wt MgO} \rightarrow 2\left(Al_2Si_2O_5(OH)_4\right)\text{(kaolinite)} + SiO_2\text{(Quartz)} + Y(Y = 2 + \alpha)\cdot MgO + 2\cdot H_2O\text{(vappor)} \quad (6)$$

$$2\left(Al_2Si_2O_5(OH)_4\right)\text{ (kaolinite)} + SiO_2\text{(Quartz)} + Y\cdot MgO \rightarrow 2(Al_2Si_2O_7)\text{ (metakaolinite)} + SiO_2\text{ (Quartz)} + Y\cdot MgO \quad (7)$$

Exothermic peaks occurring at 930–1000, 1192–1280, and 1320–1380 °C are due to the formation of the spinel, $\mu$ cordierite, and $\alpha$ cordierite phases, respectively, as shown in Eqs. 8, 9, and 10.

$$2(Al_2Si_2O_7)\text{(metakaolinite)} + SiO_2\text{(Quartz)} + Y\cdot MgO \rightarrow Si_3Al_4O_{12}\text{(Al}-\text{Si spinel)} + SiO_2\text{(amorphous)} + SiO_2\text{(Quartz)} + Y\cdot MgO \quad (8)$$

$$Si_3Al_4O_{12}\text{(Al}-\text{Si spinel)} + SiO_2\text{(amorphous)} + SiO_2\text{(Quartz)} + Y\cdot MgO \rightarrow \text{mullite}(Al_{4.5}Si_{1.5}O_{9.74}) + \text{Quartz}\ (SiO_2) + \text{sapphirine}\ (Mg_{19.12}Al_{45.24}Si_{11.64}O_{80}) + \text{magnesium silicate} \rightarrow \text{sapphirine} + \text{magnesium silicate}\ (Mg_2SiO_4) + \text{cristobalite} + \mu\ \text{cordierite}\ (Mg_4Al_8Si_{10}O_{36}) \quad (9)$$

$$\text{sapphirine} + \text{magnesium silicate} + \text{cristobalite} + \mu\ \text{cordierite} \rightarrow \text{sapphirine} + \text{magnesium silicate} + \alpha\ \text{cordierite}\ (Mg_4Al_8Si_{10}O_{36}) \quad (10)$$

The formation of $\mu$ and $\alpha$ cordierite phases in the temperature ranges 1192–1280 and 1320–1380 °C, respectively, agrees with the conclusion reached by de Almeida [1] that cordierite obtained from kaolin waste, talc, and MgO, started to form at 1250 °C and intensified at 1350 °C. Additionally, it supports the fact that $\mu$ cordierite commonly forms at low temperature and then transforms to $\alpha$ cordierite with the increase in temperature [2]. The absolute peak temperature $T_p$ decreased from 1236 to 1235 and 1231, with the increase in MgO content from 0 to 4 and 8 mass%, for $\mu$ cordierite, and from 1361 to 1291 and 1288 for $\alpha$ cordierite. In addition to lowering the absolute peak temperature $T_P$, for the formation of $\alpha$ cordierite, the increase in magnesia content retarded the crystallization of $\mu$ cordierite from the amorphous phase, as can be clearly seen from the DTA curves presented in Fig. 3.

Figure 4 shows the influence of heating rate (10, 20, 30, 40, and 50 °C $min^{-1}$) on DTA curves of DT00M, DT04M, and DT08M powders heated from 920 to 1400 °C. It can be clearly seen that the increase in heating rate, from 10 to 50 °C $min^{-1}$, resulted in shifting the position of the exothermic peak to higher temperature. DTA curves of the three samples showed the presence of four exothermic peaks between 920 and 1400 °C. Peaks between 920 and 1050 °C are characteristic of the spinel phase. The second series of exothermic peaks, between 1050 and 1200 °C,

Author's personal copy



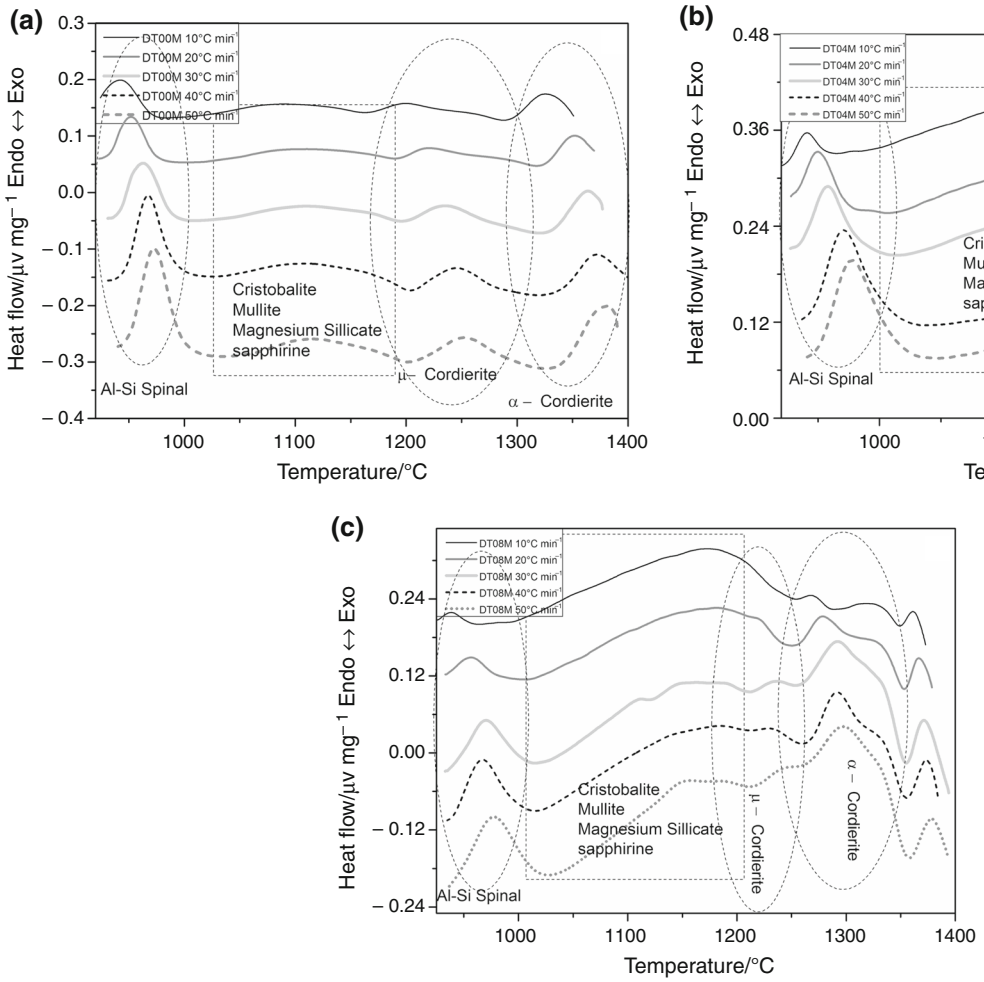


**Fig. 4** DTA curves of **a** DT00M, **b** DT04M, and **c** DT08M samples heated at different heating rates between 920 and 1400 °C

correspond to formation of various phases including cristobalite, mullite, sapphirine, and magnesium silicate. The two exothermic peaks in the range 1200–1260 and 1260–1360 °C are associated with the formation of $\mu$ and $\alpha$ cordierite phases, respectively.

Figures 5 and 6 show values of $Y$ plotted against $(1/T_p)$ for $\mu$ and $\alpha$ cordierite phases, respectively. The obtained activation energies are shown in Table 3 and presented in Fig. 7. Energies for the formation of $\mu$ cordierite in DT00M stoichiometric sample, calculated using Kissinger, Boswell, and Ozawa equations, were 577, 589, and 573 kJ mol$^{-1}$, respectively, i.e., an average of 580 kJ mol$^{-1}$, while for the formation of $\alpha$ cordierite, the values were 612, 625, and 607 kJ mol$^{-1}$, respectively, i.e., an average of 615 kJ mol$^{-1}$. The average values for the activation energies for the formation of $\mu$ and $\alpha$ cordierite, calculated from values presented in Table 3, were 726 and 948 kJ mol$^{-1}$ for DT04M sample, and 795 and 848 kJ for DT08M sample. This indicates that the activation energy for the formation of $\mu$ cordierite increased with the increase in MgO content, while for the formation of $\alpha$ cordierite, the activation energy increased with the increase in MgO content (sample DT04M) and then decreased with further increase in MgO content (sample DT08M). Figure 7 shows that, for the same sample, activation energies calculated by Kissinger, Boswell, and Ozawa methods are very close. However, large difference was observed when magnesia content was changed.

Depending on the method of calculation and MgO content, the obtained activation energies were between 573 and 964 kJ mol$^{-1}$, and the average values of the activation energies for the formation of $\mu$ and $\alpha$ cordierite were in the range 580–795 and 615–948 kJ mol$^{-1}$, respectively. The variation in the energy of formation of cordierite observed in this work supports the fact that methods of calculation and the presence of sintering aids greatly affect the energy of cordierite formation.

It is worth mentioning here that researchers [8, 29–31, 34–37] who investigated cordierite formation by non-isothermal DTA reported large variation in the energy

Author's personal copy



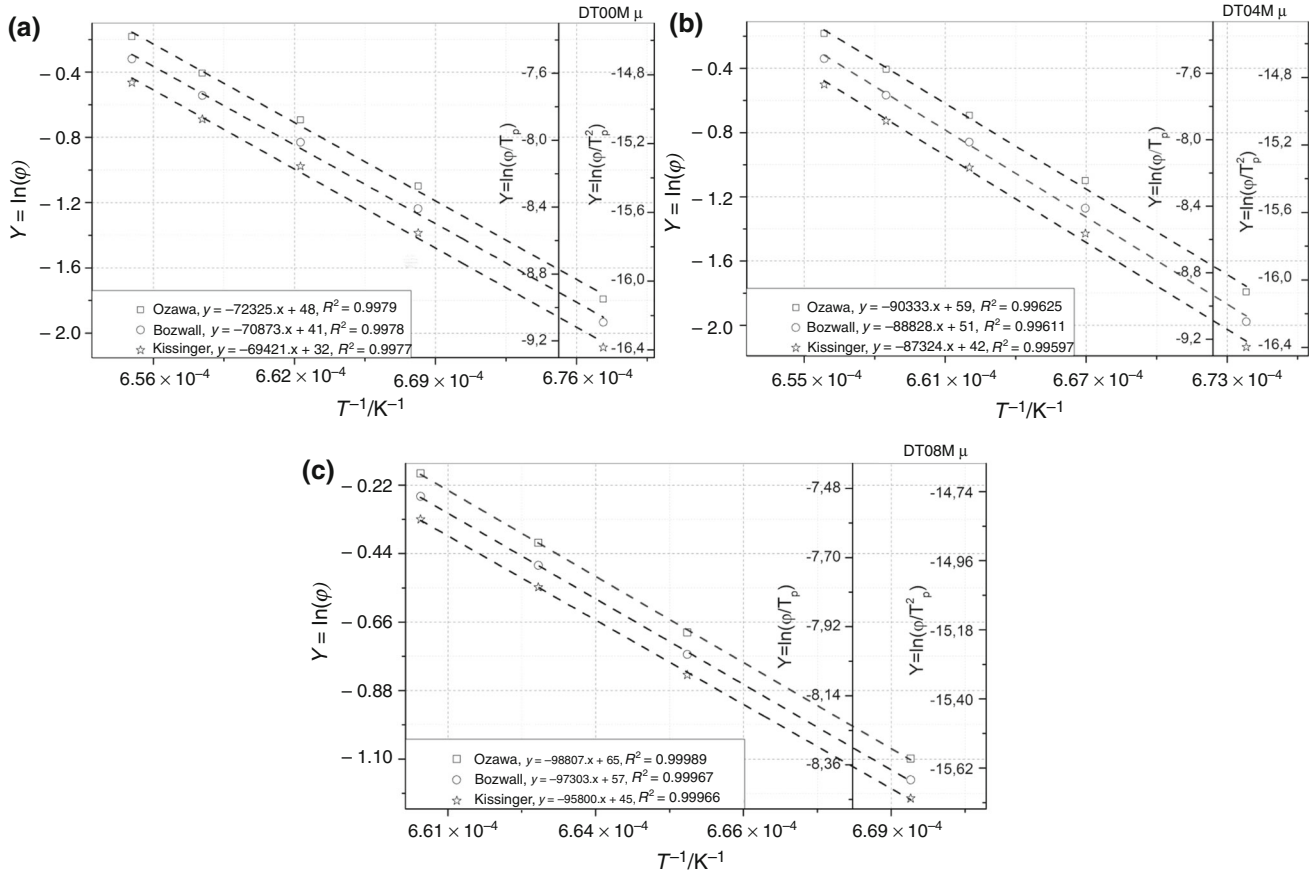


**Fig. 5** Plots of $Y\left(Y=\ln(\varphi), \ln\left(\frac{\varphi}{T_p}\right), \ln\left(\frac{\varphi}{T_p^2}\right)\right)$ versus $(1/T_p)$ of $\mu$ cordierite formation at different heating rates in **a** DT00M, **b** DT04M, and **c** DT08M samples

of formation. Donald [35] analyzed cordierite formation in a mixture of fine particle (particle size less than 45 μm and between 45 and 212 μm) of $Al_2O_3$, $SiO_2$, and MgO. He reported energy values in the range 532–574 and 399–426 kJ mol$^{-1}$ for the formation of $\mu$ and α cordierite phases, respectively. Average energies of 653 and 418 kJ mol$^{-1}$ were reported for cordierite crystallization from $CeO_2$-free and $CeO_2$-doped glasses, respectively [29]. Goel et al. [37] studied the formation of cordierite in $TiO_2$-doped MgO–$Al_2O_3$–$SiO_2$ glass and found that the activation energy values for the formation of $\mu$ and α cordierite phases were 340 and 498 kJ mol$^{-1}$, respectively. Cordierite formation energy values of 366 and 290–487 kJ mol$^{-1}$ were obtained from measurements taken on BaO-free and BaO-doped samples, respectively [31]. Silva et al. [34] crystallized cordierite from diphasic gels and reported an energy value of 467 kJ mol$^{-1}$. The crystallization of cordierite in NiO-added glass samples was investigated. and energies of 300 and 500 kJ mol$^{-1}$ were obtained for the formation of $\mu$ and α cordierite, respectively [30]. Song et al. [36] used potassium and feldspar to prepare a glass from which cordierite was crystallized. The authors obtained activation energy values between 230.77 and 279.81 kJ mol$^{-1}$ for the formation of α cordierite and between 348.85 and 374.33 kJ mol$^{-1}$ for the formation of α cordierite along with leucite. Başaran et al. prepared cordierite ceramic materials from industrial waste and reported activation energy value of 410 kJ mol$^{-1}$ [46] for cordierite crystallized in the MgO–$Al_2O_3$–$SiO_2$–$TiO_2$ glass system, and values of 336, 218, and 170 kJ mol$^{-1}$ [47] for cordierite crystallized in the same system with $Bi_2O_3$ added at 2.5, 5, and 10 mass% of, respectively.

The large variation in the reported activation energy values was attributed to the: (1) nature and composition of precursors used to obtain cordierite, (2) type of processes used to synthesize cordierite, (3) conditions under which cordierite forms, i.e., isothermal or non-isothermal, and (4) presence of sintering aids to facilitate the formation of cordierite.

The values of the kinetic parameter $n$ for the formation of $\mu$ and α cordierite phases, calculated using Eq. 4, are presented in Table 4 and 5, respectively.

Author's personal copy



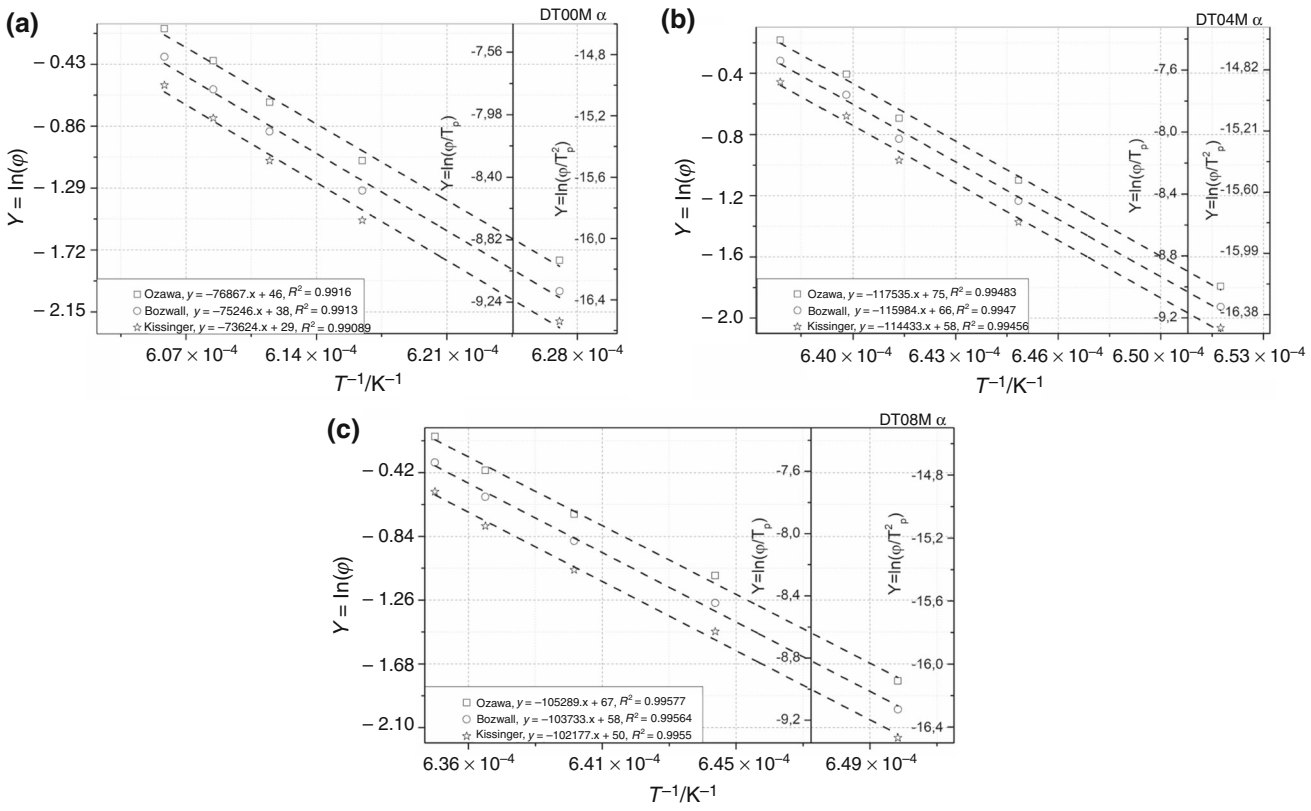


**Fig. 6** Plots of $Y\left(Y=\ln(\varphi), \ln\left(\frac{\varphi}{T_p}\right), \ln\left(\frac{\varphi}{T_p^2}\right)\right)$ versus $(1/T_p)$ of α cordierite formation at different heating rates in **a** DT00M, **b** DT04M, and **c** DT08M samples

**Table 3** Activation energy values (kJ $mol^{-1}$) for cordierite formation

| Samples | μ cordierite | | | α cordierite | | |
|---|---|---|---|---|---|---|
| | Kissinger | Boswell | Ozawa | Kissinger | Boswell | Ozawa |
| DT00M | 577 | 589 | 573 | 612 | 625 | 607 |
| DT04M | 727 | 738 | 714 | 951 | 964 | 929 |
| DT08M | 796 | 807 | 781 | 849 | 862 | 832 |

Plots of ln $(\varphi^n/T_p^2)$ versus $1/T_p$, from Eq. 5, for the formation of μ and α cordierite phases are presented in Figs. 8 and 9, respectively. A summary of the kinetic parameters $n$ and $m$ (slope of the function) is shown in Table 6.

Table 6 shows that for the stoichiometric cordierite ceramic sample (DT00M), the values of the $n$ and $m$ parameters, for the formation of μ cordierite, are close to 2. "This indicates that bulk nucleation with a constant number of nuclei was the dominant mechanism of crystallization, followed by two-dimensional growth controlled by interface reaction" [38]. However, these values were close to 3 for the formation of α cordierite, which means that the formation α cordierite is followed by three-dimensional growth. For the non-stoichiometric cordierite ceramic samples (DT04M and DT08M), the values of the $n$ and $m$ parameters, for the formation of μ cordierite, are close to 3. "This indicates that bulk nucleation with a constant number of nuclei was the dominant mechanism of crystallization, followed by three-dimensional growth" [38]. These values were close to 2 for the formation of α cordierite, which implies that the formation α cordierite is followed by two-dimensional growth. It can be concluded that the excess magnesia changed cordierite crystal behavior, and a similar trend was observed in stoichiometric (Ni, Mg) cordierite glass–ceramics as a result of substitution of nickel for magnesium [25].

## Densification

The influence of temperature and magnesia content on the bulk density and open porosity of samples sintered for 2 h is shown in Figs. 10 and 11, respectively. In the temperature range 900–1200 °C, the bulk density of DT00M

Author's personal copy



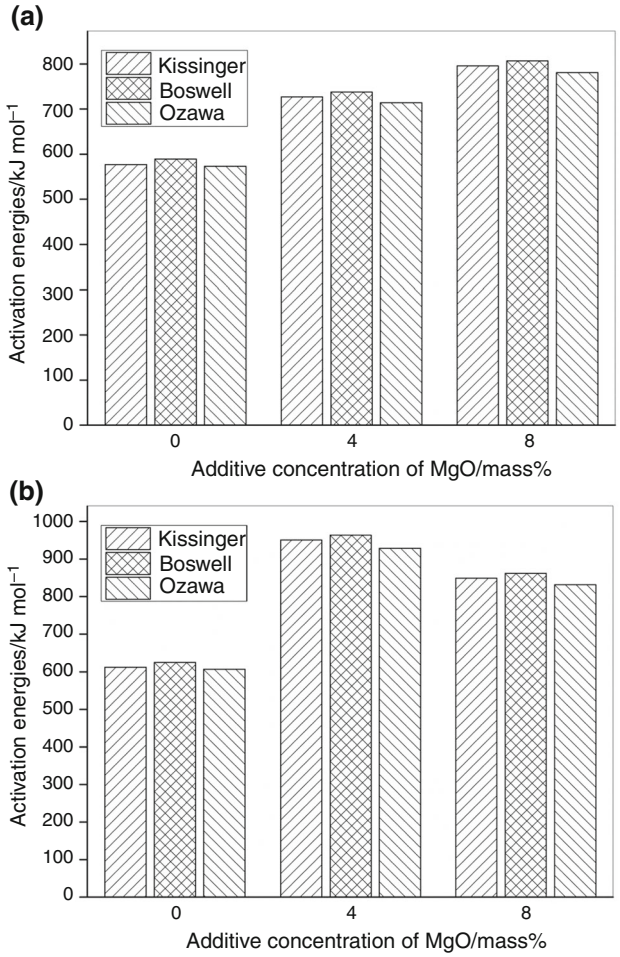


**Fig. 7** Energy of formation of **a** $\mu$ and **b** $\alpha$ cordierite

stoichiometric sample gradually increased from 2.11 g cm$^{-3}$ to reach a maximum value of 2.51 g cm$^{-3}$ and then slightly decreased to 2.50 and 2.46 g cm$^{-3}$ at 1250 and 1300 °C, respectively. The density increased because of the decrease in porosity as is clearly shown in Fig. 11. The maximum value of 2.51 g cm$^{-3}$ reached at 1200 °C is comparable to the theoretical density of cordierite [1]; this indicates the presence of almost fully dense cordierite phase at this temperature. The slight decrease in bulk density and increase in porosity at 1250 and 1300 °C may be attributed to either overfiring and formation of small amount of liquid phase or presence of a glassy phase [48]. A similar decrease in bulk density and increase in porosity was observed at 1400 °C by Njoya et al. [2] who prepared cordierite-based ceramic materials from kaolin (30 mass%), bauxite (40 mass%), and talc (30 mass%) raw materials.

For the DT04M non-stoichiometric sample, in the temperature range 900–1150 °C, its density increased from 2.21 g cm$^{-3}$ to reach 2.57 g cm$^{-3}$ at 1150 °C, slightly decreased to 2.50 at 1200 °C, and remained almost unchanged at 1250 and 1300 °C. For the DT08M non-stoichiometric sample, its density increased from 2.28 to 2.6 g cm$^{-3}$, in the temperature range 900–1150 °C, and then decreased to 2.50, 2.48, and 2.49 g cm$^{-3}$ at 1200, 1250 and 1300 °C, respectively. Figures 10 and 11 show that the three samples had similar densification behavior. The bulk density increased with the increase in temperature to reach maximum values and then slightly decreased with further increase in temperature because of the change in the

**Table 4** Kinetic parameter $n$ for $\mu$ cordierite formation

| Heating rate/°C min$^{-1}$ | DT00M | | | DT04M | | | DT08M | | |
|---|---|---|---|---|---|---|---|---|---|
| | $\Delta T$ | $T_p$ peak | $n$ | $\Delta T$ | $T_p$ peak | $n$ | $\Delta T$ | $T_p$ peak | $n$ |
| 10 | 34 | 1203 | 2.30 | 19 | 1211 | 3.31 | 17 | 1206 | 3.35 |
| 20 | 35 | 1222 | 2.29 | 20 | 1227 | 3.21 | 18 | 1221 | 3.23 |
| 30 | 40 | 1236 | 2.04 | 21 | 1238 | 3.10 | 19 | 1231 | 3.10 |
| 40 | 43 | 1244 | 1.92 | 22 | 1246 | 2.99 | 20 | 1237 | 2.97 |
| 50 | 47 | 1253 | 1.78 | 23 | 1253 | 2.89 | 21 | 1243 | 2.85 |

**Table 5** Kinetic parameter $n$ for $\alpha$ cordierite formation

| Heating rate/°C min$^{-1}$ | DT00M | | | DT04M | | | DT08M | | |
|---|---|---|---|---|---|---|---|---|---|
| | $\Delta T$ | $T_p$ peak | $n$ | $\Delta T$ | $T_p$ peak | $n$ | $\Delta T$ | $T_p$ peak | $n$ |
| 10 | 27 | 1322 | 3.20 | 24 | 1262 | 2.14 | 26 | 1265 | 2.22 |
| 20 | 29 | 1347 | 3.07 | 25 | 1277 | 2.09 | 28 | 1280 | 2.10 |
| 30 | 30 | 1361 | 3.02 | 27 | 1286 | 1.96 | 30 | 1290 | 1.99 |
| 40 | 31 | 1370 | 2.95 | 28 | 1291 | 1.9 | 31 | 1296 | 1.94 |
| 50 | 33 | 1376 | 2.80 | 29 | 1296 | 1.85 | 32 | 1300 | 1.89 |

Author's personal copy



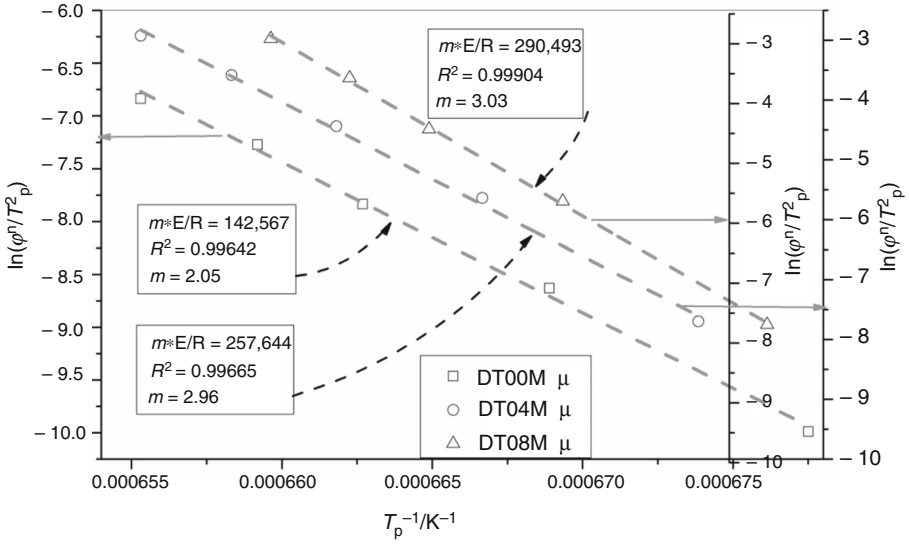


**Fig. 8** Plot of $\ln(\varphi^n/T_p^2)$ versus $1/T_p$ (Eq. 5) of $\mu$ cordierite formation as function of MgO content (DT00M, DT04M, and DT08M samples)

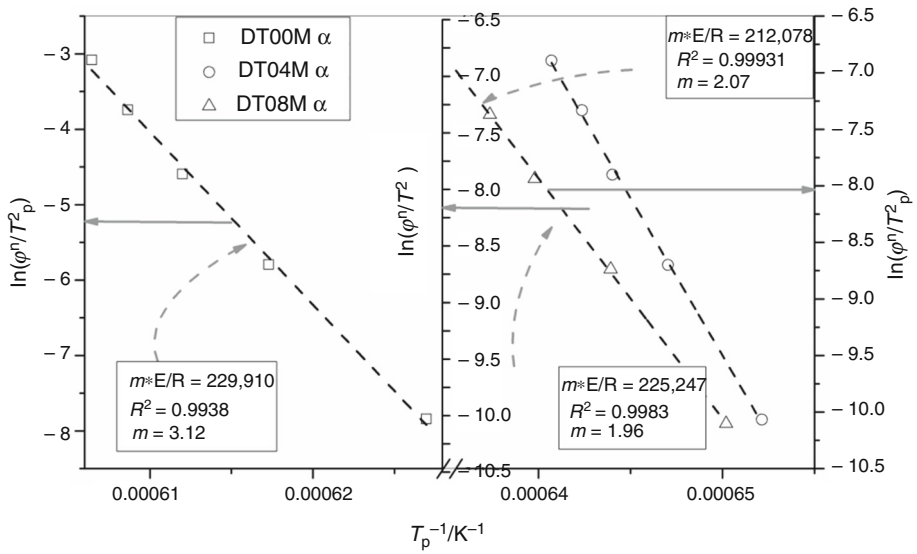


**Fig. 9** Plot of $\ln(\varphi^n/T_p^2)$ versus $1/T_p$ (Eq. 5) of $\alpha$ cordierite formation as function of MgO content (DT00M, DT04M, and DT08M samples)

**Table 6** A summary of the average values of the kinetic parameters $n$ and $m$

| Samples | $\mu$ cordierite | | $\alpha$ cordierite | |
|---|---|---|---|---|
| | $n$ | $m$ | $n$ | $m$ |
| DT00M | 2.06 | 2.05 | 3 | 3.12 |
| DT04M | 3.1 | 2.96 | 1.99 | 1.96 |
| DT08M | 3.08 | 3.03 | 2.03 | 2.07 |

number and fraction of phases as revealed by XRD and DTA results. The obtained density values are close to those reported by other researchers, who synthesized cordierite ceramics, such as 2.58 and 2.52 g $cm^{-3}$ [48], 2.4 g $cm^{-3}$ [49], 2.33 g $cm^{-3}$ [50], 2.58 g $cm^{-3}$ [51], and 2.63 g $cm^{-3}$ [2].

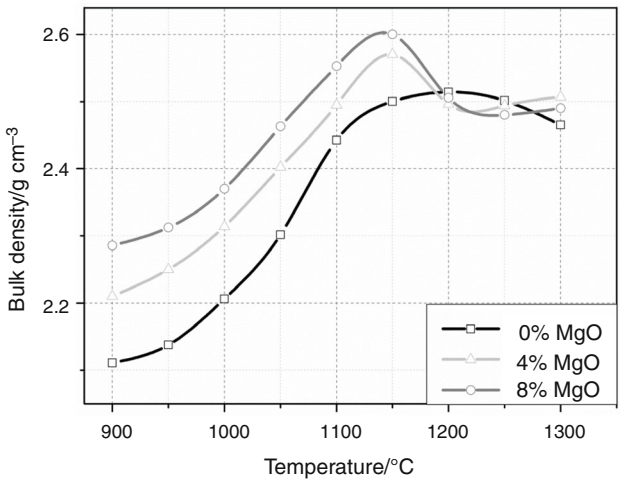


**Fig. 10** Bulk density of sintered samples

Author's personal copy



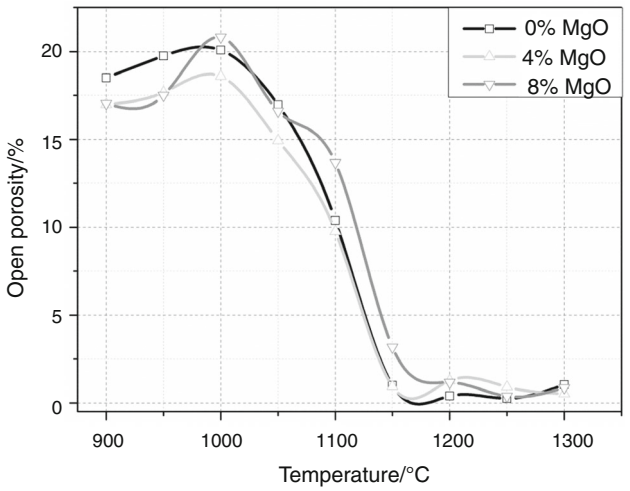


**Fig. 11** Open porosity in sintered samples

The properties of cordierite ceramic materials depend not only on the properties of the individual phases but also on their volume fraction. In this work, the reaction sintering process was successfully used to synthesize either single-phase stoichiometric cordierite or non-stoichiometric cordierite ceramics containing cordierite along with magnesium silicate and sapphirine phases. This work focused on processing and phase transformation kinetics, and the mechanical behavior and physical properties of the synthesized materials will be reported in future works.

## Conclusions

Cost-effective stoichiometric and non-stoichiometric cordierite ceramics were synthesized by reaction sintering two naturally occurring Algerian kaolinite precursors and synthetic magnesia. The formed phases and phase transformation kinetics were characterized using XRD and DTA. The energy of cordierite formation was calculated by Kissinger, Boswell, and Ozawa equations. The Augis–Bennett and Matusita equations were used to calculate the mode of crystallization ($n$) and dimension of growth ($m$) parameters, respectively. From this work, the authors concluded the following:

(1) The synthesized materials showed similar phase transformations, which finally led to the formation of cordierite in stoichiometric kaolinite–magnesia mixture, and cordierite along with other phases in kaolinite–magnesia mixture containing excess magnesia.

(2) The energy of formation of $\alpha$ cordierite was higher than that of $\mu$ cordierite. Activation energies for both $\mu$ and $\alpha$ cordierite in the non-stoichiometric samples were higher than those in the stoichiometric sample.

(3) The activation energy was less sensitive to the calculation method; however, it changed significantly with MgO content. Activation energies between 573 and 964 kJ $mol^{-1}$ were obtained.

(4) Magnesia changed the crystallization mode and crystal growth dimension. The kinetic parameters $n$ and $m$, for the formation of $\mu$ or $\alpha$ cordierite, had values between 2 and 3.

## References

1. de Almeida EP, de Brito IP, Ferreira HC, de Lucena Lira H, de Lima Santana LN, de Araújo Neves G. Cordierite obtained from compositions containing kaolin waste, talc and magnesium oxide. Ceram Int. 2018;44:1719–25.
2. Njoya D, Elimbi A, Fouejio D, Hajjaji M. Effects of two mixtures of kaolin–talc–bauxite and firing temperatures on the characteristics of cordierite- based ceramics. J Build Eng. 2016;8:99–106.
3. Rohan P, Neufuss K, Matejicek J, Dubsky J, Prchlik L, Holzgartner C. Thermal and mechanical properties of cordierite, mullite and steatite produced by plasma spraying. Ceram Int. 2004;30:597–603.
4. Hipedinger NE, Scian AN, Aglietti EF. Magnesia–ammonium phosphate-bonded cordierite refractory castables: phase evolution on heating and mechanical properties. Cem Concr Res. 2004;34:157–64.
5. Dong Y, Feng X, Dong D, Wang S, Yang J, Gao J, Liu X, Meng G. Elaboration and chemical corrosion resistance of tubular macro-porous cordierite ceramic membrane supports. J Membr Sci. 2007;304:65–75.
6. Mukhopadhyay B, Holdaway MJ. Cordierite-garnet-sillimanite-quartz equilibrium: I. New experimental calibration in the system $FeO–Al_2O_3–SiO_2–H_2O$ and certain P-T-$XH_2O$ relations. Contrib Mineral Petrol. 1994;116:462–72.
7. Sembiring S, Simanjuntak W, Situmeang R, Riyanto A, Sebayang K. Preparation of refractory cordierite using amorphous rice husk silica for thermal insulation purposes. Ceram Int. 2016;42:8431–7.
8. Boudchicha MR, Rubio F. Achour S, Synthesis of glass ceramics from kaolin and dolomite mixture. Int J Miner Metall Mater. 2017;24:194–201.
9. Wang W, Shin Z, Wang X, Fan W. The phase transformation and thermal expansion properties of cordierite ceramics prepared using drift sands to replace pure quartz. Ceram Int. 2016;42:4477–85.
10. Kobayashi Y, Sumi K, Kato E. Preparation of dense cordierite ceramics from magnesium compounds and kaolinite without additives. Ceram Int. 2000;26:739–43.
11. Sumi K, Kobayashi Y, Kato E. Synthesis and sintering of cordierite from ultrafine particles of magnesium hydroxide and kaoline. J Am Ceram Soc. 1998;80:1029–32.
12. Lee SJ, Kriven WM. Crystallization and densification of nanosize amorphous cordierite powder prepared by a PVA solution-polymerisation route. J Am Ceram Soc. 1998;81:2605–12.
13. Oh JR, Imai H, Hirashima H. Effect of Al/Si ratio on crystallization of cordierite ceramics prepared by the sol–gel method. J Ceram Soc Jpn. 1997;105:43–7.
14. Okuyama M, Fukui T, Sakurai C. Effect of complex precursors on alkoxide-derived cordierite powder. J Am Ceram Soc. 1992;75:153–60.

Author's personal copy




15. Shi ZM, Liang ZM, Zhang Q, Gu SR. Effect of cerium addition on phase transformation and microstructure of cordierite ceramics prepared by sol–gel. J Mater Sci. 2001;36:5227–30.
16. Adylov GT, Akbarov RY, Singh S, Zufarov MA, Voronov GV, Kulagina NA, Mansurova EP, Rumi MK. Crystallisation of $\mu$- and $\alpha$-cordierite in glass obtained via melting by concentrated radiant flux. Appl Sol Energy. 2008;44:135–8.
17. Hwang SP, Wu JM. Effect of composition on microstructural development in $MgO–Al_2O_3–SiO_2$ glass–ceramics. J Am Ceram Soc. 2012;84:1108–12.
18. Sumi K, Kobayashi Y, Kato E. Low-temperature fabrication of cordierite ceramics from kaolinite and magnesium hydroxide mixtures with boron oxide additives. J Am Ceram Soc. 1999;82:783–5.
19. Goren R, Gocmez H, Ozgur C. Synthesis of cordierite powder from talc diatomite and alumina. Ceram Int. 2006;32:407–9.
20. Fotoohi B, Blackburn S. Study of phase transformation and microstructure in sintering of mechanically activated cordierite precursors. J Am Ceram Soc. 2012;95:2640–6.
21. Sembiring S, Simanjuntak W, Situmeang R, Riyanto A, Karo-Karo P. Effect of alumina addition on the phase transformation and crystallisation properties of refractory cordierite prepared from amorphous rice husk silica. J Asian Ceram Soc. 2017;5:186–92.
22. Kuscer D, Bantan I, Hrovat M, Malič B. The microstructure, coefficient of thermal expansion and flexural length of cordierite ceramics prepared from alumina with different particle sizes. J Eur Ceram Soc. 2017;37:739–46.
23. Aşkın A, Tatar İ, Kılınç Ş, Tezel Ö. The utilization of waste magnesite in the production of the cordierite ceramic. Energy Proc. 2017;107:137–43.
24. Raghdi A, Heraiz M, Sahnoune F, Saheb N. Mullite–zirconia composites prepared from halloysite reaction sintered with boehmite and zirconia. Appl Clay Sci. 2017;146:70–80.
25. Miller ME, Misture ST. Stoiciometric (Ni, Mg)-cordierite glass–ceramics. J Am Ceram Soc. 2010;93:1018–24.
26. Clark SM. The kinetic analysis of irreversible consecutive solid state reactions: the effect of zinc on the formation of cordierite. J Am Ceram Soc. 2017;100:2525–32.
27. Watanabe K, Giess EA. Crystallization kinetics of high-cordierite glass. J Non-Cryst Solids. 1994;169:306–10.
28. Rudolph T, Pannhorst W, Petzow G. Determination of activation energies for the crystallization of a cordierite-type glass. J Non-Cryst Solids. 1993;155:273–81.
29. Kim DB, Lee KH. Crystallization and sinterability of cordierite-based glass powders containing $CeO_2$. J Mater Sci. 1994;29:6592–8.
30. Goel A, Shaaban ER, Ribiero MJ, Melo FCL, Ferreira JMF. Influence of NiO on the crystallization kinetics of near stoichiometric cordierite glasses nucleated with $TiO_2$. J Phys Condens Matter. 2007;19:386231.
31. Hu Y, Tsai HT. The effect of BaO on the crystallization behaviour of a cordierite-type glass. Mater Chem Phys. 1998;52:184–8.
32. Banjuraizah J, Mohamad H, Ahmad ZA. Thermal expansion coefficient and dielectric properties of non-stoichiometric cordierite compositions with excess MgO mole ratio synthesized from mainly kaolin and talc by the glass crystallization method. J Alloys Compd. 2010;494:256–60.
33. Banjuraizah J. Densification and crystallization of nonstoichiometric cordierite glass with excess MgO synthesized from kaolin and talc. J Am Ceram Soc. 2011;94:687–94.
34. Silva NT, Nasciemento NF, Cividanes LS, Bertran CA, Thim GP. Kinetics of cordierite crystallisation from diphasic gels. J Sol–Gel Sci Technol. 2008;47:140–7.
35. Donald IW. The crystallization kinetics of a glass based on the cordierite composition studied by DTA and DSC. J Mat Sci. 1995;30:904–15.
36. Song L, Wu J, Li Z, Hao X, Yu Y. Crystallization mechanisms and properties of $\alpha$-cordierite glass–ceramics from $K_2O–MgO–Al_2O_3–SiO_2$ glasses. J Non-Cryst Solids. 2015;419:16–26.
37. Goel A, Shaaban ER, Melo FCL, Ribeiro MJ, Ferreira JMF. Non-isothermal crystallization kinetic studies on $MgO–Al_2O_3–SiO_2–TiO_2$ glass. J Non-Cryst Solids. 2007;353:2383–91.
38. Redaoui D, Sahnoune F, Heraiz M, Saheb N. Phase formation and crystallization kinetics in cordierite ceramics prepared from kaolinite and magnesia. Ceram Int. 2018;44:3649–57.
39. Coats AW, Redfern JP. Kinetic parameters from thermogravimetric data. Nature. 1964;201:68–9.
40. Augis JA, Bennet JE. Calculation of Avrami parameters for heterogeneous solid-state reactions using a modification of Kissinger method. J Therm Anal Calorim. 1978;13:283–92.
41. Boswell PG. On the calculation of activation energies using modified Kissinger method. J Therm Anal. 1980;18:353–8.
42. Ozawa T. A new method for analysing thermogravimetric data. Bull Chem Soc Jap. 1965;38:1881–6.
43. Ptáček P, Šoukal F, Opravil T, Havlica J, Brandštetr J. Crystallization of spinel phase from metakaoline: the non isothermal thermos dilatometric CRH study. Powder Technol. 2013;243:40–5.
44. Romero M, Martín-Márquez J, Rincón JM. Kinetic of mullite formation from a porcelain stoneware body for tiles production. J Eur Ceram Soc. 2006;26:1647–52.
45. Sanad MMS, Rashad MM, Abdel-Aal EA, Powers K. Novel cordierite nanopowders of new crystallization aspects and its cordierite-based glass ceramics of improved mechanical and electrical properties for optimal use in multidisciplinary scopes. Mater Chem Phys. 2015;162:299–307.
46. Başaran C, Canikoğlu N, Toplan HÖ, Toplan N. The crystallization kinetics of the $MgO–Al_2O_3–SiO_2–TiO_2$ glass ceramics system produced from industrial waste. J Therm Anal Calorim. 2016;125:695–701.
47. Başaran C, Toplan N, Toplan HÖ. The crystallization kinetics of the $Bi_2O_3$-added $MgO–Al_2O_3–SiO_2–TiO_2$ glass ceramics system produced from industrial waste. J Therm Anal Calorim. 2018;134:313–21.
48. Tunç Tuğba, Şükran Demirkıran A. The effects of mechanical activation on the sintering and microstructural properties of cordierite produced from natural zeolite. Powder Technol. 2014;260:7–14.
49. Bejjaoui R, Benhammou A, Nibou L, Tanouti B, Bonnet JP, Yaacoubi A, Ammar A. Synthesis and characterization of cordierite ceramic from Moroccan stevensite and andalusite. Appl Clay Sci. 2010;49:336–40.
50. Fotoohi B, Blackburn S. Effects of mechanochemical processing and doping of functional oxides on phase development in synthesis of cordierite. J Eur Ceram Soc. 2012;32:2267–72.
51. Neto JBR, Moreno R. Effect of mechanical activation on the rheology and casting performance of kaolin/talc/alumina suspensions for manufacturing dense cordierite bodies. Appl Clay Sci. 2008;38:209–18.